J Electr Eng Technol.2017; 12(6): 2099-2105
http://doi.org/10.5370/JEET.2017.12.6.2099

ISSN(Print) 1975-0102
ISSN(Online) 2093-7423

Adaptive Gain-based Stable Power Smoothing of a DFIG

Hyewon Lee*, Min Hwang*, Jinsik Lee, Eduard Muljadi***, Hong-Ju Jung§ and Yong Cheol Kang†**

Abstract – In a power system that has a high wind penetration, the output power fluctuation of a large-scale wind turbine generator (WTG) caused by the varying wind speed increases the maximum frequency deviation, which is an important metric to assess the quality of electricity, because of the reduced system inertia. This paper proposes a stable power-smoothing scheme of a doubly-fed induction generator (DFIG) that can suppress the maximum frequency deviation, particularly for a power system with a high wind penetration. To do this, the proposed scheme employs an additional control loop relying on the system frequency deviation that operates in combination with the maximum power point tracking control loop. To improve the power-smoothing capability while guaranteeing the stable operation of a DFIG, the gain of the additional loop is modified with the rotor speed and frequency deviation. The gain is set to be high if the rotor speed and/or frequency deviation is large. The simulation results based on the IEEE 14-bus system demonstrate that the proposed scheme significantly lessens the output power fluctuation of a WTG under various scenarios by modifying the gain with the rotor speed and frequency deviation, and thereby it can regulate the frequency deviation within a narrow range.

Keywords: Frequency deviation, Kinetic energy, Power fluctuation, Power smoothing, Rotor speed, and stable operation

1. Introduction

For a power grid that has a high penetration level of wind power, regulating the system frequency within a narrow range is a crucial challenge [1, 2]. This is because variable-speed wind turbine generators (WTGs), such as doubly-fed induction generators (DFIGs), and fully-rated converter-based WTGs perform maximum power point tracking (MPPT) control, which is unable to mitigate the fluctuating output power of the WTGs caused by the continuously varying wind speeds. To minimize these problems, some countries specify requirements on the ramp rates of the output power of a wind power plant (WPP) [3].

Power-smoothing schemes of WTGs can be divided in two groups: those with or without energy storage systems (ESSs) [4-8]. In [4-6], ESSs such as flywheels, super-capacitors, or batteries were suggested to smooth the frequency fluctuation caused by WTGs. ESSs help mitigate the frequency fluctuation by releasing or absorbing energy; however, these devices require an extra cost for installation and maintenance, particularly for a large-scale WTG.

To avoid or reduce the additional cost for the ESS, power-smoothing schemes were suggested that release or absorbs the kinetic energy stored in the rotating masses of a WTG. These schemes use additional control loops operating in conjunction with the MPPT control loop: the rate of change of frequency (ROCOF) loop and/or frequency deviation loop [7, 8]. These loops help smooth the output power fluctuation; however, these schemes use the fixed gain for additional control loops. A large gain can improve the power-smoothing capability of a WTG, but it is unable to ensure stable operation in the low-rotor-speed region; thus, to avoid this, the use of a small gain is inevitable, thereby providing a limited contribution to mitigating the frequency fluctuation.

This paper proposes a stable power-smoothing scheme of a DFIG to regulate the frequency deviation within a narrow range. The proposed scheme uses an additional control loop relying on the frequency deviation operating in conjunction with the MPPT control loop. To improve the power-smoothing capability while ensuring the stable operation of a DFIG, the gain of the additional control loop varies with on the rotor speed and frequency deviation. The performance of the proposed scheme is investigated under continuously varying wind conditions for two wind power penetration levels in the IEEE 14-bus system using an EMTP-RV simulator.

---

† Corresponding Author: Dept. of Electrical Engineering, WeGAT Research Center, and Smart Grid Research Center, Chonbuk National University, Korea. (yckang@jbnu.ac.kr)
* Dept. of Electrical Engineering and WeGAT Research Center, Chonbuk National University, Korea. ({hyewonlee, skyway333}@jbnu.ac.kr)
** Korea Electric Association (KEA), Korea. (jinsiklee@kea.kr).
*** National Renewable Energy Laboratory (NREL), USA. (eduard.muljadi@nrel.gov)
§ Power & Industrial Systems R&D Center Hyosung Corporation, Korea. (seaworld@hyosung.com)

Received: February 26, 2017; Accepted: June 20, 2017

Copyright ⓒ The Korean Institute of Electrical Engineers
This is an Open-Access article distributed under the terms of the Creative Commons Attribution Non-Commercial License (http://creativecommons.org/licenses/by-nc/3.0/) which permits unrestricted non-commercial use, distribution, and reproduction in any medium, provided the original work is properly cited.

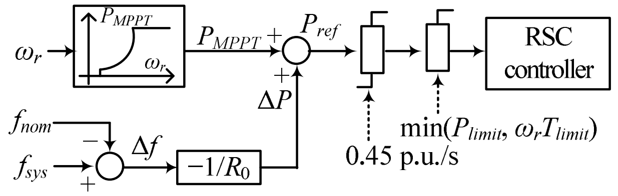

ω_r: rotor speed
f_{nom}, f_{sys}: nominal frequency and system frequency
P_{limit}, T_{limit}: active power limit and torque limit

Fig. 1. Conventional power-smoothing scheme in [8]

2. Conventional Power-smoothing Scheme in [8]

For regulating the system frequency within a narrow range, conventional power-smoothing schemes of a DFIG rely on ROCOF and/or frequency deviation (Δf) [7, 8]. The ROCOF loop is prone to noise components contained in the measured system frequency. Thus, the proposed scheme uses the Δf loop only as in the conventional scheme in [8]. This section briefly describes the features of the conventional scheme in [8].

Fig. 1 shows the conventional scheme of a DFIG in [8]. The power reference (P_{ref}) consists of the output of the MPPT control (P_{MPPT}) and the output of the Δf loop (ΔP) as in:

$$P_{ref} = P_{MPPT} + \Delta P \tag{1}$$

To extract maximum power from the wind, the reference for P_{MPPT} is set to (2), as in [9]:

$$P_{MPPT} = k_g \omega_r^3 \tag{2}$$

where k_g is a constant and set to 0.512 in this paper.

In the conventional scheme, ΔP in (1) is determined as:

$$\Delta P = -\frac{1}{R_0}\Delta f \tag{3}$$

where $1/R_0$ is the fixed gain of the Δf loop and is set to 25 in this paper.

3. Proposed Power-smoothing Scheme using the Adaptive Gain Depending on ω_r and Δf

The proposed scheme aims to improve the power-smoothing capability of a DFIG while ensuring stable operation. To achieve this objective, the proposed scheme uses the adaptive gain of the Δf loop ($K(\omega_r, \Delta f)$), which is modified with ω_r and Δf, as shown in Fig. 2.

In the proposed scheme, ΔP is determined as:

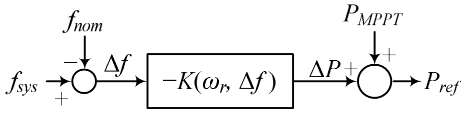

(a) Proposed power-smoothing scheme

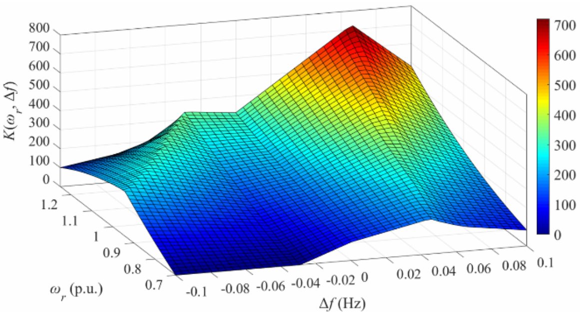

(b) $K(\omega_r, \Delta f)$ in the three-dimensional space

Fig. 2. Proposed frequency-regulating scheme of a DFIG

$$\Delta P = \begin{cases} -K_{low}(\omega_r, \Delta f)\Delta f, & for\ f_{sys} \le 60\text{ Hz} \\ -K_{high}(\omega_r, \Delta f)\Delta f, & for\ f_{sys} > 60\text{ Hz} \end{cases} \tag{4}$$

where $K_{low}(\omega_r, \Delta f)$ and $\mathrm{K}_{\mathrm{high}}(\omega_r, \Delta f)$ are the gains of the Δf loop defined in the lower and higher frequency region than the nominal frequency, respectively.

K_{low} and K_{high} are determined as in:

$$\left.\begin{aligned} K_{low}(\omega_r, \Delta f) &= C_0(\omega_r^2 - \omega_{\min}^2)(-a\Delta f + 1) \quad && for\ \Delta f \le 0 \\ K_{high}(\omega_r, \Delta f) &= C_0\omega_r^2(a\Delta f + 1), && for\ \Delta f > 0 \end{aligned}\right\} \tag{5}$$

where C_0 and a are the constants and are set to 200 and 20, respectively. C_0 and a can be determined in many ways depending on the design purposes and system conditions. A larger value of C_0 can be used to increase ΔP at any ω_r and Δf. In contrast, a larger value of a can be used to increase the contribution of the Δf term in (5).

Note that K_{low} and K_{high} are set to be proportional to ($\omega_r^2 - \omega_{\min}^2$) and ω_r^2, respectively; this means that the gain becomes large if there exists a large amount of kinetic energy is stored; otherwise, the gain becomes small. The reason for this is as follows. To mitigate the frequency fluctuation, a DFIG should release the kinetic energy in the lower frequency region to increase the frequency, but absorb the kinetic energy in the higher frequency region to reduce the frequency. In addition, to prevent over-deceleration of a DFIG in the lower frequency region, K_{low} is set to zero at $\omega_r = \omega_{\min}$.

To suppress the large frequency deviation, the magnitude of K_{low} and K_{high} increases as the magnitude of Δf increases. The increase rate depends on a. This means that a can be set to be large to attain the high power-smoothing capability as Δf increases. Thus, the proposed scheme can significantly mitigate the frequency fluctuation as Δf increases.

To prevent P_{ref} from reaching the output power limit of a DFIG, this paper considers the gain limit ($K_{low\_limit}(\omega_r, \Delta f)$ and $K_{high\_limit}(\omega_r, \Delta f)$), as in:

$$\left.\begin{aligned} K_{low\_limit}(\omega_r,\Delta f) &= \frac{\min(P_{limit},\omega_r T_{limit}) - P_{MPPT}}{\Delta f} \quad & for\ \Delta f \le 0 \\ K_{high\_limit}(\omega_r,\Delta f) &= \frac{P_{MPPT} - 0.04\,p.u.}{\Delta f} \quad & for\ \Delta f > 0 \end{aligned}\right\} \tag{6}$$

where K_{low_limit} and K_{high_limit} are the gain limit in the lower- and higher-frequency than 60 Hz (the nominal frequency), respectively; and P_{limit} and T_{limit} are the active power limit and torque limit, respectively.

For the negative Δf, K_{low_limit} allows P_{ref} to reach min (P_{limit}, $\omega_r T_{limit}$). For the positive Δf, K_{high_limit} allows P_{ref} to reach 0.04 p.u., which is a minimum power output of a DFIG [10].

Finally, the gain is set as the minimum value between the gains in (5) and (6) for all ω_r and Δf.

4. Model system

Fig. 3 shows the IEEE 14-bus system used to demonstrate the performance of the proposed power-smoothing scheme using an EMTP-RV simulator. The system includes five synchronous generators, static loads, and two aggregated DFIG-based WPPs.

The operating conditions of the synchronous generators in [11] are shown in Fig. 3. The droop gains of all of the synchronous generators are set to 5%. To simulate a power system that has a low ramping capability, they are all assumed to be steam turbine generators; the steam turbine governor model is the IEEEG1 steam governor model [12]. The total static load is set to approximately 600 MW and 57.4 MVAr.

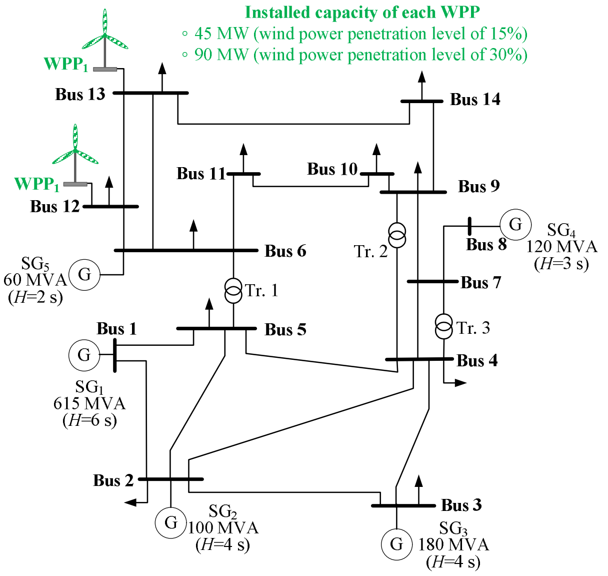

Fig. 3. IEEE 14-bus system with three WPPs

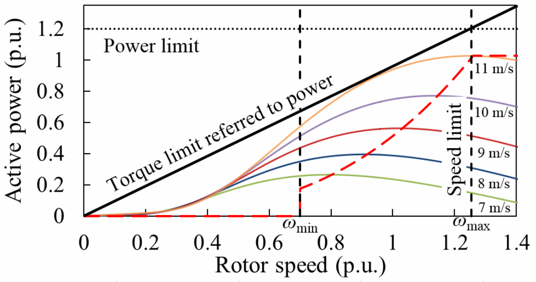

Fig. 4. Input-output power characteristics of a DFIG

A pitch-angle controller used in this paper prevents ω_r from exceeding the maximum operating limit ($\omega_{\max}$). In addition, a pitch-angle controller includes the rate and angle limiters, which are set to ±10°/s and 30°, respectively [13]. For the frequency-regulating scheme, the rapid and excessive increase of output power may cause mechanical stresses [14]. To avoid these, this paper considers the torque, power, and rate limits, as shown in Fig. 4. P_{limit} and T_{limit} are set to 1.20 p.u. and 1.17 p.u., respectively [15]. The rate limit is set to 0.45 p.u./s [16]. The operating range of ω_r is between 0.7 p.u. ($\omega_{\min}$) and 1.25 p.u. ($\omega_{\max}$). The rated, cut-in, and cut-out speeds of the DFIG are set to 11 m/s, 4 m/s, and 25 m/s, respectively.

5. Case studies

The system frequency of a power grid with a high wind penetration might fluctuate because of the varying wind speed. This section investigates the performance of the power-smoothing schemes under the scenarios by continuously varying the wind speeds for the wind power penetration levels set to 15% and 30%, which indicate the installed capacity of each WPP of 45 MW and 90 MW, respectively (see Table 1). In this paper, the wind power penetration level is defined as the installed capacity of a WPP divided by the load [17].

Fig. 5 shows the input wind speeds of two WPPs, which have the same pattern with the different average wind speeds of 8 m/s for Case 1 (the red line) and 11 m/s for Case 2 (the blue line). The input wind speeds are typical wind data given by an EMTP-RV simulator [18]. The performance of the proposed scheme is compared to that of the conventional scheme in [8] and to a case that performs MPPT operation. In all schemes, if ω_r reaches $\omega_{\max}$, a pitch-angle controller is activated. In the following subsections, "+" and "–" indicate the regions where Δf is

Table 1. Information on case studies

	Case 1	Case 2
Installed capacity of each WPP (MW)	45	90
Wind power penetration level (%)	15	30
Average of input wind speed (m/s)	8	11

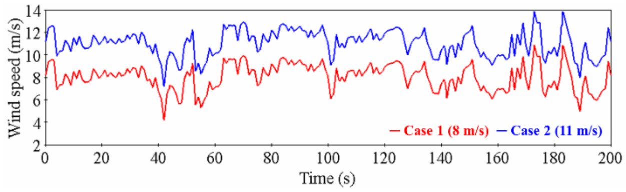

Fig. 5. Input wind speeds for Case 1 and Case 2

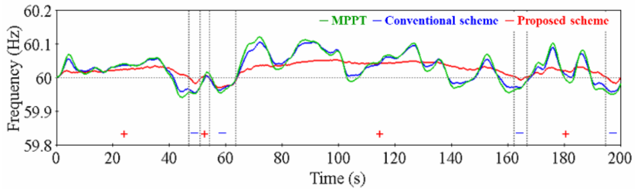

(a) Frequency

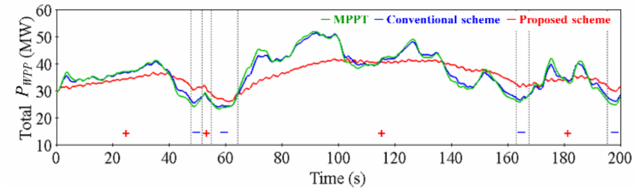

(b) Total output power of two WPPs

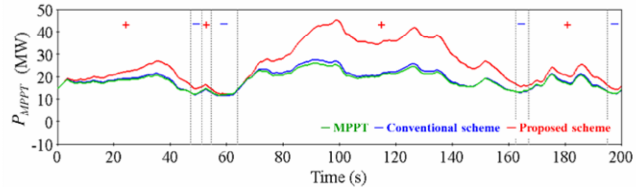

(c) P_{MPPT} of WPP$_1$

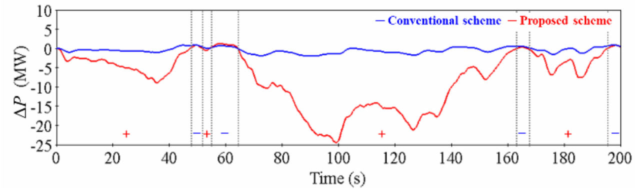

(d) ΔP of WPP$_1$

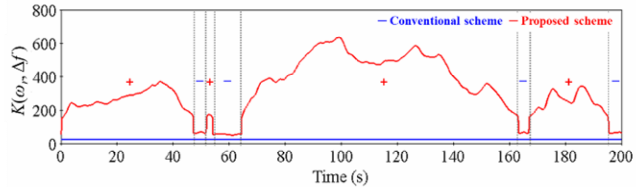

(e) $K(\omega_r, \Delta f)$ of WPP$_1$

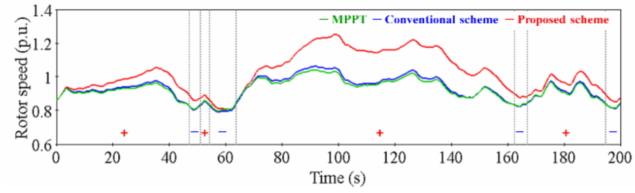

(f) Rotor speed of WPP$_1$

Fig. 6. Results for Case 1

positive and negative, respectively.

5.1 Case 1: wind power penetration level of 15% and average wind speed of 8 m/s

Fig. 6 shows the results for Case 1, in which the average wind speed is 8 m/s for two WPPs. As shown in Fig. 6(a), in the proposed scheme the frequency fluctuation is significantly mitigated compared to the conventional scheme because the proposed scheme significantly smooths the total output power of the WPPs by adjusting the control gain with ω_r and Δf (see Fig. 6(b)). Around 100 s, the wind speed decreases; thus, the output power of WPPs decreases in MPPT operation and the conventional scheme; however, the proposed scheme suppresses the frequency decrease more than the conventional scheme by releasing the kinetic energy of a WTG (see Figs. 6(a) and 6(b)).

As shown in Table 2, the root mean square (RMS) values of Δf in the conventional and proposed schemes are 92% and 58% of that of MPPT operation, respectively. In addition, the maximum Δf in the conventional and proposed schemes are 88% and 43% of that of MPPT operation, respectively; in contrast, the minimum Δf in the conventional and proposed schemes are 79% and 53% of that of MPPT operation, respectively. This means that the proposed scheme provides better performance of regulating the frequency deviation in the higher frequency region than in the lower frequency region. This is because K_{high} in (5) is larger than K_{low}.

As shown in Fig. 6(d), ΔP in the proposed scheme is larger than that in the conventional scheme because $K(\omega_r, \Delta f)$ in the proposed scheme is significantly larger than that in the conventional scheme (see Fig. 6(e)). Thus, ω_r in the proposed scheme varies more widely than it does in the conventional scheme; this means that the proposed scheme utilizes the variation range of ω_r more than the conventional scheme.

In this case, the generated energy in the proposed scheme, the conventional scheme, and an MPPT operation is 1.9675 MWh, 2.0315 MWh, and 2.0317 MWh, respectively. The generated energy in the proposed scheme is 3.16% less than that in an MPPT operation. This is because in this case the period under the over-frequency region is longer than that in the under-frequency region and thus a DFIG should reduce its output power to suppress the positive frequency deviation. Note that the reduced energy

Table 2. Quantitative results for Case 1

	MPPT operation	Conventional scheme	Proposed scheme
RMS {Δf} (Hz)	0.052	0.048	0.030
Maximum Δf (Hz)	0.120	0.105	0.052
Minimum Δf (Hz)	−0.060	−0.047	−0.031
Variation range of ω_r for WPP$_1$ (p.u.)	0.243	0.274	0.411

is not the loss, but it is stored in the form of the kinetic energy in the rotating masses of a DFIG. ω_r in the proposed scheme at 200 s is 0.874 p.u., which is larger than that at 0 s by 0.0118 p.u.; in contrast, ω_r in an MPPT operation at 200 s is 0.847 p.u., which is smaller than that at 0 s by 0.0147 p.u.

5.2 Case 2: wind power penetration level of 30% and average wind speed of 11 m/s

This subsection investigates the performance of the power-smoothing schemes for a higher wind power penetration level than Case 1. Fig. 7 shows the results for Case 2. In this case, the frequency fluctuation is more severe than it is in Case 1 because of a higher wind power penetration level. As in Case 1, the frequency fluctuation is significantly mitigated compared to the conventional scheme (see Fig. 7(a)). In addition, in this case the proposed scheme can smooth the frequency fluctuation more than it does in Case 1 (see Figs. 6(a) and 7(a)). This is because the output power fluctuation of WPPs is smoothed.

The proposed scheme provides better performance to smoothing the frequency fluctuation in the higher frequency region than in the lower frequency region. The RMS values of Δf in the conventional and proposed schemes are 72% and 19% of that of MPPT operation, respectively. The maximum Δf in the conventional and proposed schemes are 66% and 8% of that of MPPT operation, respectively; and the minimum Δf in the conventional and proposed schemes are 69% and 28% of that of MPPT operation, respectively. Further, the proposed scheme provides better contribution to lessening the frequency fluctuation as the wind speed increases.

As in Case 1, in the proposed scheme ω_r varies more widely than it does in the conventional scheme. In all schemes, the pitch-angle controller is activated.

In Case 2, the generated energy in the proposed scheme, the conventional scheme, and an MPPT operation is 8.608 MWh, 9.055 MWh, and 9.207 MWh, respectively. The generated energy in the proposed scheme is 6.5% less than that in an MPPT operation. The reduced energy in the proposed scheme in Case 2 is larger than that in Case 1. This is because in this case, the pitch-angle controller is activated and thus the mechanical energy from the wind is reduced; in addition, the pitch angle in the proposed scheme is larger than that in an MPPT operation. As a result, unlike Case 1, ω_r in the proposed scheme at 200 s is 1.082 p.u., which is smaller than that in an MPPT operation (1.158 p.u.). However, the reduced energy caused by using the pitch-angle controller can be paid back from the transmission system operators (TSOs) as a reward of providing a contribution on mitigating the system frequency deviation. However, this issue is beyond the scope of this paper because an incentive system for mitigating the frequency deviation depends on the TSOs.

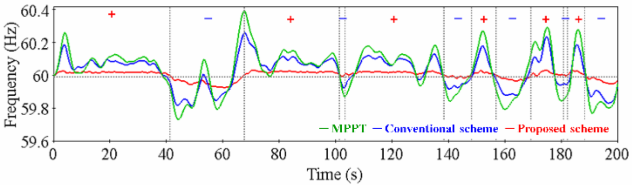

(a) Frequency

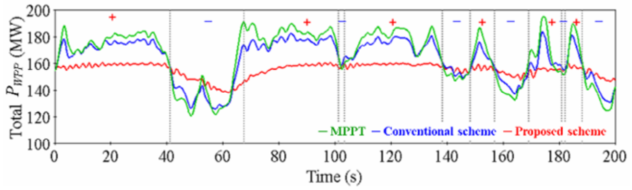

(b) Total output power of two WPPs

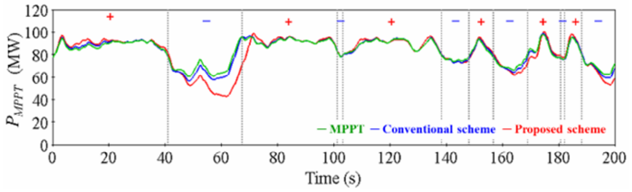

(c) P_{MPPT} of WPP$_1$

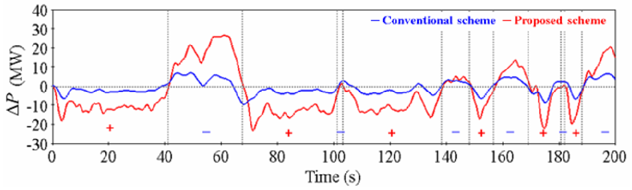

(d) ΔP of WPP$_1$

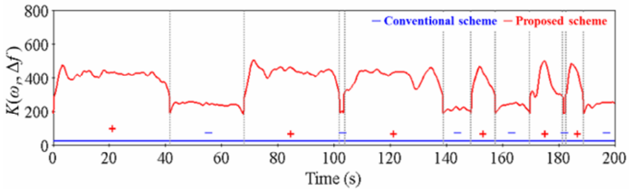

(e) $K(\omega_r, \Delta f)$ of WPP$_1$

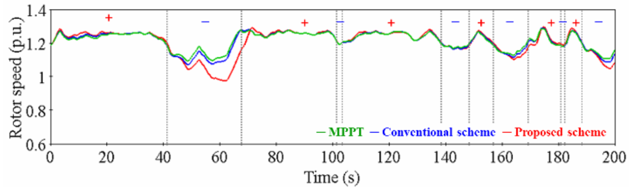

(f) Rotor speed of WPP$_1$

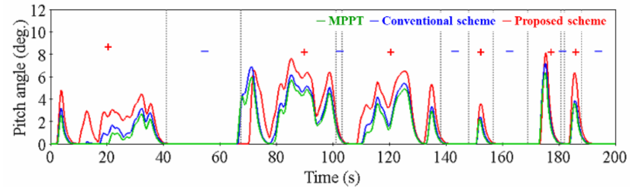

(g) Pitch angle of WPP$_1$

Fig. 7. Results for Case 2

Table 3. Quantitative results for Case 2

	MPPT operation	Conventional scheme	Proposed scheme
RMS {Δf} (Hz)	0.139	0.100	0.026
Maximum Δf (Hz)	0.392	0.260	0.030
Minimum Δf (Hz)	−0.270	−0.187	−0.076
Variation range of ω_r for WPP$_1$ (p.u.)	0.192	0.219	0.321

6. Conclusion

This paper proposes a stable power-smoothing scheme of a DFIG relying on the frequency deviation loop, the gain of which is adjusted depending on ω_r and Δf. To improve the power-smoothing capability of a DFIG, the control gain in the higher frequency region is set to be larger than that in the lower frequency region. Further, the gain increases as the magnitude of Δf increases.

Simulation results indicate that the proposed scheme significantly smooths the output power fluctuation of a DFIG by adjusting the control gain of the frequency deviation loop, thereby improving the power-smoothing capability of a DFIG caused by varying wind speeds. In addition, the proposed scheme shows better performance when the wind speed increases and/or wind power penetration level is high.

Appendix

Table A. Load consumption of the IEEE 14-bus system

Bus #	1	2	3	4	5	6	7
P (MW)	-	43.3	188.0	95.2	14.5	71.6	-
Q (MVAr)	-	11.4	15.1	−1.2	1.1	4.5	-
Bus #	8	9	10	11	12	13	14
P (MW)	-	57.0	17.3	6.6	35.2	34.4	35.5
Q (MVAr)	-	12.4	4.3	1.3	0.8	4.1	3.6

Acknowledgements

This work was supported in part by the National Research Foundation of Korea (NRF) grant funded by the Korea government (MSIP) (No. 2010-0028509) and in part by the New & Renewable Energy Core Technology Program of the Korea Institute of Energy Technology Evaluation and Planning (KETEP) granted financial resource from the Ministry of Trade, Industry & Energy, Republic of Korea (No. 20123010020160).

References

[1] H. Bevrani, *Robust Power System Frequency Control*, 2nd ed. New York: Springer, 2014.

[2] I. M. de Alegría, J. Andreu, J. L. Martín, P. Ibañez, J. L. Villate, and H. Camblong, "Connection requirements for wind farms: A survey on technical requirements and regulation," *Renew. Sust. Energ. Rev.*, vol. 11, no. 8, pp. 1858-1872, Oct. 2007.

[3] E. Fagan, S. Grimes, J. McArdle, P. Smith, and M. Stronge, "Grid code provisions for wind generators in Ireland," in *Proc. 2005 IEEE PES General Meeting*, vol. 2, San Francisco, California, pp. 1241-1247.

[4] F. Díaz-González, F. D. Bianchi, A. Sumper, and O. Gomis-Bellmunt, "Control of a flywheel energy storage system for power smoothing in wind power plants," *IEEE Trans. Energy Convers.*, vol. 29, no. 1, pp. 204-214, Mar. 2014.

[5] J. Pegueroles-Queralt, F. D. Bianchi, and O. Gomis-Bellmunt, "A power smoothing system based on supercapacitors for renewable distributed generation," *IEEE Trans. Ind. Electron.*, vol. 62, no. 1, pp. 343-350, Jan. 2015.

[6] L. Xiangjun, H. Dong, and L. Xiaokang, "Battery energy storage station (BESS)-based smoothing control of photovoltaic (PV) and wind power generation fluctuations," *IEEE Trans. Sust. Energy*, vol. 4, no. 2, pp. 464-473, Apr. 2013.

[7] I. D. Margaris, S. A. Papathanassiou, N. D. Hatziargyriou, A. D. Hansen, and P. Sørensen, "Frequency control in autonomous power systems with high wind power penetration," *IEEE Trans. Sust. Energy*, vol. 3, no. 2, pp. 189-199, Apr. 2012.

[8] M. Wang-Hansen, R. Josefsson, and H. Mehmendovic, "Frequency controlling wind power modeling of control strategies," *IEEE Trans. Sust. Energy*, vol. 4, no. 4, pp. 954-959, Oct. 2013.

[9] B. Shen, B. Mwinyiwiwa, Y. Zhang, and B. Ooi, "Sensorless maximum power point tracking of wind by DFIG using rotor position phase lock loop (PLL)," *IEEE Trans. Power Electron.*, vol. 24, no. 4, pp. 942-951, Apr. 2009.

[10] B. Shen, B. Mwinyiwiwa, Y. Zhang, and B. Ooi, "Sensorless maximum power point tracking of wind by DFIG using rotor position phase lock loop (PLL)," *IEEE Trans. Power Electron.*, vol. 24, no. 4, pp. 942-951, Apr. 2009.

[11] J. Sutter, J. Maleche, and C. Muriithi, "Analysis of power system transient stability due to increased integration of geothermal power," presented at the 39th Workshop on Geothermal Reservoir Engineering, Stanford, California, Feb. 24-26, 2014.

[12] R. T. Byerly, O. Aanstad, D. H. Berry, R. D. Dunlop, D. N. Ewart, B. M. Fox, L. H. Johnson, and D. W. Tschappat, "Dynamic models for steam and hydro turbines in power system studies," *IEEE Trans. Power App. Syst.*, vol. PAS-92, pp. 1904-1915, Nov. 1973.

[13] M. H. Hansen, A. Hansen, T. J. Larsen, S. Øye, P. Sørensen, and P. Fuglsang, "Control design for a pitch-regulated, variable speed wind turbine," Risø National Laboratory, Risø, Denmark, Tech. Rep. Risø-R-1500(EN), Jan. 2005.

[14] Y. Wang, G. Delille, H. Bayem, X. Guilaud, and B.

Francois, “High wind power penetration in isolated power systems — Assessment of wind inertial and primary frequency responses,” *IEEE Trans. Power Syst.*, vol. 28, no. 3, pp. 2412-2420, Aug. 2013.

[15] J. M. Mauricio, A. Marano, A. Gómez-Expósito, and J. L. M. Ramos, “Frequency regulation contribution through variable-speed wind energy conversion systems,” *IEEE Trans. Power Syst.*, vol. 24, no. 1, pp. 173-180, Feb. 2009.

[16] K. Clark, N. W. Miller, and J. J. Sanchez-Gasca, “Modeling of GE wind turbine-generators for grid studies,” Version 4.5, Apr. 16, 2010.

[17] T. Ackermann, *Wind Power in Power Systems*, 2nd ed. England: John Wiley & Sons, Ltd., 2012.

[18] Electromagnetic Transient Program, EMTP-RV, CEA Technologies, Inc., 2017. [Online]. Available: http://www.emtp-software.com.

Hyewon Lee She received the B.Sc. degree from Chonbuk National University, Jeonju, Korea in 2010. She is studying for her Ph.D. degree at Chonbuk National University and also an assistant researcher of the wind energy grid-adaptive technology (WeGAT) Research Center supported by the Ministry of Science, ICT, and Future Planning (MSIP), Korea. Her research interest is development of wind energy grid integration techniques.

Min Hwang He received the B.Sc. and M.Sc. degrees from Chonbuk National University, Jeonju, Korea in 2015 and 2017, respectively. He is also an Assistant Researcher with the Wind energy Grid-Adaptive Technology (WeGAT) Research Center supported by the Ministry of Education, Science, and Technology, Korea. His research interests include control systems for wind power plants.

Jinsik Lee He received the B.Sc. and M.Sc. degrees from Chonbuk National University, Jeonju, Korea in 2011 and 2013, respectively. Currently, he is pursuing the Ph.D. degree at Chonbuk National University. He is an Assistant Researcher with the Wind energy Grid-Adaptive Technology (WeGAT) Research Center supported by the Ministry of Education, Science, and Technology, Korea. His research interests include control systems for wind power plants.

Eduard Muljadi He received the Ph.D. degree in electrical engineering from the University of Wisconsin at Madison, Madison, WI, USA. From 1988 to 1992, he taught at California State University at Fresno, Fresno, CA, USA. In 1992, he joined the National Renewable Energy Laboratory, Golden, CO, USA. His research interests include electric machines, power electronics, and power systems in general, with an emphasis on renewable energy applications. He is an Editor of the IEEE TRANSACTIONS ON ENERGY CONVERSION. He is involved in the activities of the IEEE Industry Application Society (IAS), Power Electronics Society, and Power and Energy Society (PES). He is currently a member of the Working Group on Renewable Technologies and the Task Force on Dynamic Performance of Wind Power Generation.

Hong-Ju Jung Hong-ju Jung received the B.S. and M.S. degrees in electrical engineering from Kwangwoon University, Seoul, Korea, in 1998 and 2000, respectively, and the Ph.D. degree from Hanyang University, Seoul, Korea, in 2015. Since 2000, he has been with Hyosung Corporation, where he is currently General Manager at the Hyosung Power & Industrial Systems R&D Center, Gyeonggi-do, Korea. His main research interests include power converter system for renewable energies and HVDC/FACTS converter System.

Yong Cheol Kang He received his B.Sc., M.Sc., and Ph.D. degrees from Seoul National University, Korea, in 1991, 1993, and 1997, respectively. He has been with Chonbuk National University, Korea, since 1999. He is currently a professor at Chonbuk National University and the director of the WeGAT Research Center supported by the MSIP, Korea. He is currently a Member of the International Electrotechnical Commission working group TC88/WG27. He is an Editor of the IEEE TRANSACTIONS ON SUSTAINABLE ENERGY. His research interests include the development of control techniques for wind power plants.